İSTANBUL COMMERCE UNIVERSITY

GRADUATE SCHOOL OF NATURAL AND APPLIED SCIENCES

ALTITUDE-HOLD FLIGHT CONTROLLER DESIGN OF SUPERSONIC AIRCRAFT FOR LONGITUDINAL MOTION

Ahmet Hulusi ÖZ

Supervisor
Prof. Dr. Muammer KALYON

MASTER'S THESIS
DEPARTMENT OF MECHATRONICS ENGINEERING
ISTANBUL - 2021

ACCEPTANCE AND APPROVAL PAGE

On 05/07/2021 **Ahmet Hulusi ÖZ** succefully defended the thesis, entitled **" Altitude-Hold Flight Controller Design of Supersonic Aircraft for Longitudinal Motion "** which he prepared after fulfilling the requirements specified in the associated legislations, before the jury members whose signatures are listed below. This thesis is accepted as a **MASTER'S THESIS** by Istanbul Commerce University, Graduate School of Natural and Applied Sciences **Mechatronics Engineering Department**.

Approved by:

Supervisor **Prof. Dr. Muammer KALYON**
Istanbul Commerce University

Jury Member **Assist. Prof. Dr. Vedat TAVAS**
Istanbul Commerce University

Jury Member **Assist. Prof. Dr. İlker ÜSTOĞLU**
Istanbul Technical University

Approval Date : 29/07/2021

Istanbul Commerce University, Graduate School of Natural and Applied Sciences, accordance with the 2nd article of the Board of Directors Decision dated 29/07/2021 and numbered 2021/317, "Ahmet Hulusi ÖZ" who has determined to fulfill the course load and thesis obligation was unanimously decided to graduated.

Prof. Dr. Necip ŞİMŞEK
Head of Graduate School of Natural and Applied Sciences

DECLERATION OF CONFORMITY IN ACADEMIC AND ETHIC CODES

Istanbul Commerce University, Institute of Science, thesis writingin accordance with the rules of this thesis study,

- I have obtained all the information and documents in the thesis under the academic rules,
- I give all information and results in a visual, auditory and written manner in accordance with scientific code of ethics,
- in the case that the works of others are used, I have found the works in accordance with the scientific norms,
- I show all of the works I have cited as a source,
- I have not tampered with the data used,
- And that did not present any part of this thesis as a dissertation study at this university or at another university

I declare.

29/07/2021

Ahmet Hulusi ÖZ

CONTENTS

ABSTRACT

M.Sc. Thesis

ALTITUDE-HOLD FLIGHT CONTROLLER DESIGN OF SUPERSONIC AIRCRAFT FOR LONGITUDINAL MOTION

Ahmet Hulusi ÖZ

İstanbul Commerce University
Graduate School of Applied and Natural Sciences
Department of Mechatronic Engineering

Supervisor: Prof. Dr. Muammer KALYON

2021, 45 Pages

This article proposes the conventional implementation of a "Altitude-Hold Controller" for a high speed hypothetical aircraft. Dynamic stability of the aircraft is established beyond longitudinal motion of the aircraft. Firstly, the static stability, which is called as Stability Augmentation System (SAS), is studied for the system. The stability conditions are analyzed and then the suitable controller design is developed over the longitudinal motion of the aircraft. The controller which is implemented to the system is designed with linear methods by linearizing the longitudinal equation of motions. Furthermore, the linearized system is also analyzed and studied over performance issue. After the characteristic of the airframe is studied, the controller design is optimized in order to get a good approximation for the overall flight system. The methods used for the design are Root-Locus Method to get the controller coefficients. The overall longitudinal motion is divided to two sections which are; the first one is the inner loop that deals with the pitching motion parameters and the second one is the outer loop that deals with the altitude reference, flight-path angle and velocity on the vertical motion of the aircraft. The simulation of the linearized longitudinal motion of the aircraft is developed in MATLAB/Simulink computer program. The analysis and the results are built and discussed with this program. In conclusion, the controller is implemented to the Simulink after the mathematical background and the control theory is finished and established for the overall system. The final results are discovered and expressed over the MATLAB/Simulink.

Keywords: Altitude-Hold control, flight control systems, flight mechanics, longitudinal motion control, pitch control.

ÖZET

Yüksek Lisans Tezi

SÜPERSONİK HAVA ARACI'NIN UZUNLAMASINA HAREKET KAPSAMINDA "İRTİFA-KİLİTLEME" UÇUŞ KONTROLCÜSÜNÜN TASARIMI

Ahmet Hulusi ÖZ

İstanbul Ticaret Üniversitesi
Fen Bilimleri Enstitüsü
Mekatronik Mühendiliği Anabilim Dalı

Danışman: Prof. Dr. Muammer KALYON

2021, 45 Sayfa

Bu makale, yüksek hızlı varsayımsal bir uçak için "İrtifa-Kilitleme Kontrolcü"sünün geleneksel uygulamasını göstermektedir. Uçağın dinamik kararlılığı, uzunlamasına hareket kapsamında elde edilmektedir. Öncelikle, sistem için Kararlılık Arttırma Sistemi (SAS) olarak adlandırılan statik kararlılık çalışılmıştır. Kararlılık koşulları analiz edilmiş ve ardından uçağın uzunlamasına hareketi üzerinden uygun kontrolcü tasarımı geliştirilmiştir. Ayrıca, doğrusallıştırılmış sistem de performans sorunu üzerinden analiz edilmiş ve incelenmiştir. Uçak gövdesinin karakteristiği incelendikten sonra, genel uçuş sistemi için iyi bir yaklaşım elde etmek adına kontrolcü tasarımı optimize edilmiştir. Tasarım için kullanılan yöntemler, kontroller katsayılarını elde etmek için Root-Locus Metodu'dur. Genel uzunlamasına hareket iki bölüme ayrılmıştır; birincisi yunuslama hareketi parametreleri ve açıları ile ilgilenen iç kontrol döngüsü, ikincisi ise uçağın dikey hareketindeki irtifa referansı, uçuş-yolu açısı ve hızı ile ilgilenen dış kontrol döngüsüdür. Uçağın doğrusallıştırılmış uzunlamasına hareketinin simülasyonu MATLAB/Simulink bilgisayar programında geliştirilmiştir. Analiz ve sonuçlar bu program üzerinden oluşturulmuş ve tartışılmıştır. Son olarak, matematiksel arka planda oluşturulan kontrolcü Simulink üzerinde uygulanmıştır ve tüm sistem için kontrol teorisi tamamlanmıştır. Nihai sonuçlar bu simülasyon üzerinden elde edilmiş ve MATLAB/Simulink üzerinden ifade edilmiştir.

Anahtar kelimeler: İrtifa-Kilitleme kontrolü, uçuş kontrol sistemleri, uçuş mekaniği, uzunlamasına hareket kontrolü, yunuslama açısı kontrolü.

ACKNOWLEDGMENTS

I would like to mention my gratitude to my supervisor Prof. Dr. Muammer KALYON, who guided me for this work and encourage me in every way of this study

I would like to thank my dear friend Mehmet Şahin, with whom I constantly exchanged ideas, had the opportunity to work together and mastered together.

Finally, I would like to thank my dear family who always have never withheld their love and support throughout my education and working life, and who always stood by me.

Ahmet Hulusi ÖZ
ISTANBUL, 2021

LIST OF FIGURES

LIST OF TABLES

Page

LIST OF ABBREVIATIONS

$\widetilde{C_D}$	Equivalent drag coefficient for level flight
$\widetilde{C_L}$	Equivalent lift coefficient for level flight
C_{D_0}	Mean Drag coefficient
$C_{D_{CL}2}$	Drag coefficient with respect to lift coefficient
$C_{D_{control\,surfaces}}$	Drag coefficient with respect to control surfaces
$C_{D_{flaps}}$	Drag coefficient with respect to flaps
C_{L_0}	Mean Lift coefficient
C_{L_α}	Lift coefficient with respect to angle of attack
$C_{L_{\delta e}}$	Lift coefficient with respect to elevator deflection
$C_{M_{\dot{\alpha}}}$	Pitching moment coefficient with respect to angle of attack rate
C_{M_0}	Mean Pitching moment coefficient
C_{M_q}	Pitching moment coefficient with respect to pitch rate
C_{M_α}	Pitching moment coefficient with respect to angle of attack
$C_{M_{\delta e}}$	Pitching moment coefficient with respect to elevator deflection
C_{N_p}	Yawing moment coefficient with respect to roll rate
C_{N_r}	Yawing moment coefficient with respect to yaw rate
C_{N_β}	Yawing moment coefficient with respect to side-slip angle
$C_{N_{\delta a}}$	Yawing moment coefficient with respect to aileron deflection
$C_{N_{\delta r}}$	Yawing moment coefficient with respect to rudder deflection
C_{Y_β}	Side-force coefficient with respect to side-slip angle
$C_{Y_{\delta r}}$	Side-force coefficient with respect to rudder deflection
C_{l_p}	Rolling moment coefficient with respect to roll rate
C_{l_r}	Rolling moment coefficient with respect to yaw rate
C_{l_β}	Rolling moment coefficient with respect to side-slip angle
$C_{l_{\delta a}}$	Rolling moment coefficient with respect to aileron deflection
$C_{l_{\delta r}}$	Rolling moment coefficient with respect to rudder deflection
C_D	Drag coefficient
C_L	Lift coefficient
C_Y	Mean Side-force coefficient
C_l	Rolling moment coefficient
C_m	Pitching moment coefficient
C_n	Yawing moment coefficient
$F_D\ (X_s)$	Drag Force
$F_L(Z_s)$	Lift Force
$F_Y(Y_s)$	Side Force
F_{wx}	Force in x-axis with respect to wind frame
F_{wy}	Force in y-axis with respect to wind frame
F_{wz}	Force in z-axis with respect to wind frame
G_{x_s}	Gravity Force in x-axis with respect to stability frame
G_{y_s}	Gravity Force in y-axis with respect to stability frame
G_{z_s}	Gravity Force in z-axis with respect to stability frame
L_s	Rolling Moment

M_s	Pitching Moment
N_s	Yawing
P_{x_s}	Propulsion Force in x-axis with respect to stability frame
P_{y_s}	Propulsion Force in x-axis with respect to stability frame
P_{z_s}	Propulsion Force in x-axis with respect to stability frame
P_x	Propulsion Force in x-axis
P_y	Propulsion Force in y-axis
P_z	Propulsion Force in z-axis
g_x	Gravity Force in x-axis
g_y	Gravity Force in y-axis
g_z	Gravity Force in z-axis
δ_a	Aileron deflection
δ_e	Elevator deflection
δ_r	Rudder deflection
m	Mass of the aircraft
$\mathrm{V_p}$	Velocity of the aircraft
g	Gravity acceleration
$RCAM$	Research Civilization Aircraft Model
α	Angle of Attack
β	Side slip angle
γ	Flight-path angle
μ	Bank angle around velocity vector

1. INTRODUCTION

The Altitude-Hold control system is one of the most important control segment for the aircrafts. It forces the overall system on a designed altitude which is a significant flight. If the aircraft is supersonic, which is like in this study, this control system is getting important. Therefore, over the years, so many control methods were developed and studied to overcome this problem. The common method is dealing with the characteristic of the longitudinal motion of the aircraft via classical methods. Some of these methods are Eigenvalue assignment which is known as pole placement method, Root-Locus method and Routh-Hurwitz Criteria. The common feature of these methods is that they has to be all built with linear mathematical background. So that, the system has to be linearized to design and develope a proper controller.

Nonlinear systems are not easy to control systems. They have highly uncertainity conditions which can not be handle or overcome with a basic control methodologies. Aircrafts are one of the hardest controllable systems. They have highly nonlinear behaviour. The states which can be observed or controlled are are all dependent of a nonlinear terms. The change of environment is also one of the cruical point to trigger this nonlinearity. In this case, the states have to be controlled with a pilot command or automatically. Mostly, linearization methods are used to control the aircraft subsystems, since the nonlinearity is not easy subject to handle.

However, some adaptivity methods are used to control the states without applying any linearity to the system. For example, dynamic inversion control is based on feedback linearization. Nonlinear Dynamic Inversion Control is also based on feedback linearization. In this study, nonlinear dynamic inversion control method is discussed in order to develop a proper and robust controller for a nonlinear system such as an aircraft.

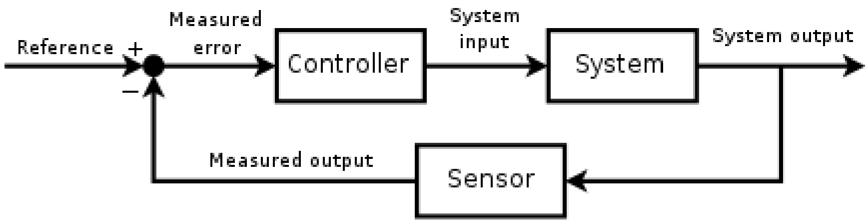

Figure 1.1 : System definition

NDI control uses the nonlinear feedback states to the controller section of the total aircraft model. It has two section or stages as an expamle on Figure 1.1 to complete the control loop. The very useful and the coolest thing than the other techniques is that it uses the wind-axes parameter as a reference inputs. This is important for the stability issue, since the parameters and states which are fed into the input side to differ from the references are the states which makes the stability control easily. They are all maint parameters to handle maneuvering the aircraft. Hence, the aircraft model is developed for the implement a controller into the working plant for this study. The model is developed on the MATLAB/Simulink program. The controller is also developed and studied on the same program. Outputs of the system is observed and analyzed.

2. LITERATURE REVIEW

Supersonic longitudinal flight control system is studied for the modern civil supersonic transport aircraft. Since the supersonic regime is increasing complex input command set and more nonlinearity for the aircraft, the stability augmentation system is also not easy to control (Steer, 2004). In this study, the set of input command response for one phase of flight, which is longitudinal flight, and handling qualities is revised.

Nonlinear Dynamic Inversion control method is implemented to a supersonic aircraft for the longitudinal motion to get handling qualities in steady conditions (Steer, 2001). The NDI control system is based on the pitch rate criteria and pitch attitude, and also the normal acceleration commands. Hence, the pitching motion response and behaviour is analyzed for a longitudinal flight control system in this study.

In another way, angle of attack can be used as an input command for the longitudinal control of a supersonic aircrafts (Lee, 2020). In order to increase the aerodynamic performance of the aircraft, static stability is analyzed. The longitudinal control law is based on dynamic inversion and proportional and integral control methods in this study.

In latest years of 70's, there are some flight experience beyond the altitude hold and mach hold autopilots on YF-12 aircraft at mach number 3 (Gilyard, 1978). The main reason is to obtain the maximum range at high altitude and high mach number. The controller is designed as two sections, which are high-pass filtered pitch rate feedback for inner loop with altitude rate proportional and integral gains and auto-throttle control for mach number conditions

Nonlinear Dynamic Inversion (NDI) control can be implemented to the system by not doing any linearization. This method is mostly used for the aircraft systems. The people which dealed with this problem with adaptive control approach of NDI used for a small unmanned aircraft systems (Harris,2017). This control method has also an incremental way to implement to the system. In this case, Incremental NDI Control was studied for a stability analysis (Veldt, 2016). The performance issue is also one of the most critical subject to deal with, since the nonlinearity can make the system unstabilize easily and damage the system. Therefore, the optimum solution or the performing the method to the system is a significant point. For this case, the performance and the structure of the method was well studied for the past years (Miller, 2013). In this study, general structure, controllability, adaptivity and the implementation of NDI control method was studied.

3. AIRFRAME MODEL OF AN AIRCRAFT

Hypothetical supersonic aircraft is evaluated for the plant model, since the behaviour of the aircraft will be shown in this study. The controller is also designed from this plant model. The mathematical representation of the plant model is explained (Howe, 1990).

3.1. Vector Equations of Motion

In the atmospheric conditions, aircraft is a rigid body moving this environment. For a x-y-z space, the aircraft has a 6 degrees of freedom whose three of them are on the translational and three of them are on the rotational form. The whole body is under effect of several forces. These forces can be explained as aerodynamic, propulsive and gravitational forces. The definitions of the behaviour of the aircraft equations are described in two sections, which are translational and rotational equations. By this two attitude of the equations, the final, general form of equations of motions are derived. The mathematical description of translational equations can be represented as:

$$\frac{md\overrightarrow{V_p}}{dt} = \sum Total\ Forces = \sum Aerodynamic + Propulsion + Gravity \qquad (3\text{-}1)$$

Where, $\boldsymbol{m}$ is the mass of the body, $\overrightarrow{\boldsymbol{V_p}}$ is the velocity vector and t is the time.
The rotational equations can be represented as :

$$\frac{d\vec{H}}{dt} = \sum Total\ Moments = \sum Aerodynamic + Propulsion \qquad (3\text{-}2)$$

Where, H is the angular momentum vector.

These descriptions are required in order to get a transfer function for building plant model and the controller. Therefore, the vector form of the equations of motions has to be rewritten in scalar form because of differenciating operations can be operated in this form. However, the axis systems have to be also considered in order to do that.

3.2. Axis System Definitions

Aircraft motion can be represented on several axes systems. Thus, the behaviour of the motion background can be analyzed and considered in terms of mathematical approach.

Since the aircraft has an acting force by aerodynamic effects and these effects are acting to the body, the first axis system should be the body axis in order to revise the motion. The body axes can be defined as x-y-z axis system on the origin of the aircraft. This system is fixed with respect to the aircraft. If the body axis system is represented in terms of mathematical approach, it will be like below:

X – Axis : is along the longitudinal direction
Y – Axis : is along the right wing direction
Z – Axis : is along the downward to origin of the body

After defining the body axes, the earth axes x_e, y_e, z_e can be defined in order to represent the motion of the aircraft on the earth axis frame. The representation of the earth axes can be derived from the body axis with respect to euler angles Φ, θ, φ shown in Figure 3.1.

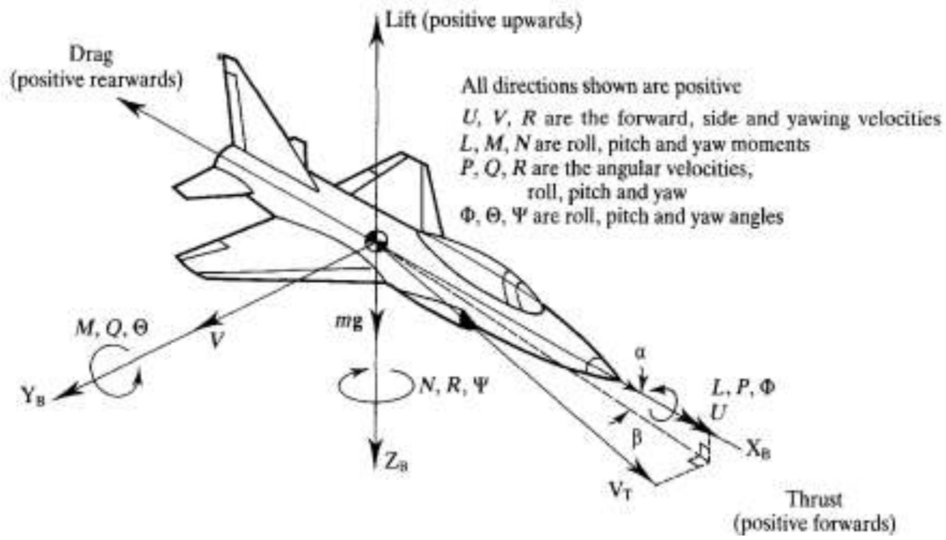

Figure 3.1 : Aircraft freebody diagram (McLean, 1990)

Since they are on the same origin, rotation of the earth axes to the body axes can be explained like below:

Firstly, x_e, y_e, z_e (earth axes) must be rotate along yawing motion with φ Euler-angle. Secondly, earth axes must be rotated along pitching motion with θ Euler-angle. Thirdly, earth axes must be rotated along rolling motion with Φ Eular-angle.

The bext axis system can be defined as stability axes which are important for building and analyzing the control system. This axis system can be also represented with respect to body axes in terms of orientation of the angle of attack, α. Therefore, the rotation from body to stability axes can be completed by rotating the axes about y-axis through the negative angle of attack.

The last axis system, wind axes, is also important for defining the behaviour of the motion of the aircraft along the parameters which are belong the wind axes system. This is also important for the same structure system of the controller. The wind axes system can be expressed as the rotation of the stabilirt axes system with the side-slip angle, β. In terms of representing of the motion, the body axes are important, and the aerodynamic moments and forces are represented on the stability axes system.

3.3. Scalar Form of Equation of Motion

In order to get the representation from vector form of equation (3-1), translational vector, has to be differantiated with respect to time. Their expressions are like below:

Firstly, the mathematical expression of this operation :

$$\frac{d\vec{R}}{dt}\bigg|i = \frac{d\vec{R}}{dt}\bigg|r \ + \ \vec{\Omega} + \vec{R} \tag{3-3}$$

Where, $\left|\frac{d\vec{R}}{dt}\right| i$ is the time rate of the position vector R viewed by the inertial frame. $\left|\frac{d\vec{R}}{dt}\right| i$ term is the same vector viewed by the rotating frame. And $\vec{\Omega}$ is the angular velocity vector of the rotating frame. Therefore, the represantation of the equations of translational and angular velocities will become in terms of the scalar form:

$$\overrightarrow{V_p} = u\vec{\imath} + v\vec{\jmath} + w\vec{k} \tag{3-4}$$

$$\vec{\Omega} = p\vec{\imath} + q\vec{\jmath} + r\vec{k} \tag{3-5}$$

Where u, v, w are linear velocities and p,q,r are angular rates, roll,pitch and yaw respectively, on the on the corresponding i,j,k unit vector of the x,y,z body axes, respectively. The time rate of the velocity vector will be:

$$\frac{d\overrightarrow{V_p}}{dt} = \frac{d\overrightarrow{V_p}}{dt}\bigg|i = \frac{d\overrightarrow{V_p}}{dt}\bigg|r + \ \vec{\Omega}x\overrightarrow{V_p} \tag{3-6}$$

In equation (3-3), the rotating frame r is for the body axis frame. For rearranging the equation (3-5) and (3-6), the following terms are obtained.

$$\frac{d\overrightarrow{V_p}}{dt}|i = (\dot{u} + qw - rv)\vec{\imath} + (\dot{v} + ru - pw)\vec{\jmath} + (\dot{w} + pv - qu)\vec{k} \tag{3-7}$$

Where the x component of equation (3-7) is equal to $\frac{F_x}{m}$, the force term on the x axis, the y component of equation (3-7) is equal to $\frac{F_y}{m}$, the force term on the y axis, the z component of equation (3-7) is equal to $\frac{F_z}{m}$, the force term on the z axis.

Hence, the force vector represents the derived forces on x,y,z axes, respectively. Since the addition of these forces must be equal to the total forces in equation (3-1), they can be subtracted from each other in order to find the $\dot{u}, \dot{v}, \dot{w}$:

$$\dot{u} = \frac{F_x}{m} - wq + vr \tag{3-8}$$

$$\dot{v} = \frac{F_y}{m} - ur + wp \tag{3-9}$$

$$\dot{w} = \frac{F_z}{m} - vp + uq \tag{3-10}$$

In equations (3-8), (3-9) and (3-10), translational state equations are derived in order to build a plant model. After defining the translational equations in body axes, the rotational terms can be expressed mathematically with illustrated by p,q,r:

$$\vec{H} = I\vec{\Omega} \tag{3-11}$$

Where, I is the mass moment of inertia matrix of the aircraft.

$$\begin{bmatrix} H_x \\ H_y \\ H_z \end{bmatrix} = \begin{bmatrix} I_{xx} & -I_{xy} & -I_{xz} \\ -I_{xy} & I_{yy} & -I_{yz} \\ -I_{xz} & -I_{yz} & I_{zz} \end{bmatrix} \begin{bmatrix} p \\ q \\ r \end{bmatrix} \tag{3-12}$$

In equation (3-12), H_x, H_y, H_z are the angular momentum x,y,z components, respectively. In order to find the moments acting to the body, the angular momentum must be differentiated with time according to inertial frame, like in equation (3-7).

$$\frac{d\vec{H}}{dt}|i = \left(I_{xx}\dot{p} - I_{xz}\dot{r} - I_{xz}pq + I_{zz}qr - I_{yy}qr\right)\vec{\imath}$$
$$+\left(I_{yy}\dot{q} + I_{xx}rp - I_{xz}r^2 + I_{xz}p^2 - I_{zz}rp\right)\vec{\jmath} \tag{3-13}$$
$$+\left(-I_{xz}\dot{p} - I_{zz}\dot{r} + I_{yy}pq - I_{xx}pq + I_{xz}rq\right)\vec{k}$$

By getting a closed form of equation (3-13), the total moments can be represented on x,y,z axes respectively.

$$\sum Total\ Moments = M_x\vec{\imath} + M_y\vec{\jmath} + M_z\vec{k} \tag{3-14}$$

The reason of these mathematical operations is to obtain the rotational state equations like it is done on the translational state equations.

$$\dot{p} = \frac{M_x}{I_{xx}} + \left(I_{yy} - I_{zz}\right) * \frac{qr}{I_{xx}} + \frac{I_{xz}}{I_{xx}}(pq - \dot{r}) \tag{3-15}$$
$$\dot{q} = \frac{M_y}{I_{yy}} + (I_{zz} - I_{xx}) * \frac{rp}{I_{yy}} + \frac{I_{xz}}{I_{yy}}(r^2 - p^2) \tag{3-16}$$
$$\dot{r} = \frac{M_z}{I_{zz}} + \left(I_{xx} - I_{yy}\right) * \frac{pq}{I_{zz}} + \frac{I_{xz}}{I_{zz}}(\dot{p} - qr) \tag{3-17}$$

The results of the equations above give the rotational state equations of the aircraft in body axes.

3.4 Aerodynamic Forces and Moments

Normally, the main principle and important term of the aerodynamic forces are aerodynamic coefficients which are all unique for each aircraft. However, there is also atmospheric effects acting to the body. When all of these effects are taken into account, the first step is the dynamic pressure term.

$$\bar{Q} = \frac{1}{2}\rho V_p^2 \tag{3-18}$$

Where ρ is the air density and V_p is the total aircraft velocity.

Then, the aerodynamic forces can be defined on the stability axes of the aircraft. If they are expressed mathematically, X_s, Y_s and Z_s become the force components with respect to x_s, y_s and z_s ,stability axes.

$$X_s = \frac{1}{2}\rho V_p^2 C_D \tag{3-19}$$

$$Y_s = \frac{1}{2}\rho V_p^2 C_Y \tag{3-20}$$

$$Z_s = \frac{1}{2}\rho V_p^2 C_L \tag{3-21}$$

Where, C_D is the drag coefficient

C_Y is the side-force coefficient

C_L is the lift coefficient

The coefficients are all dependent of other parameters. Therefore, they can be written as:

$$C_D = C_{D_0} + C_{D_{C_L^2}} C_L^2 + C_{D_{flaps}} + C_{D_{control\ surfaces}} \tag{3-22}$$

$$C_Y = C_{Y_\beta}\beta + C_{Y_{\delta_r}}\delta_r \tag{3-23}$$

$$C_L = C_{L_0} + C_{L_\alpha}\alpha + C_{L_{\delta_e}}\delta_e + C_{D_{flaps}} + C_{D_{control\ surfaces}} \tag{3-24}$$

Where, δ_e, δ_r are the control surface deflections which are the significant parameters for flight control systems.

For the same principle like aerodynamic forces, the aerodynamic moments are also dependent of dynamic pressure and moment coefficients. They can be expressed as L_s, M_s *and* N_s with respect to stabilty axes x_s, y_s *and* z_s , respectively.

$$L_s = \frac{1}{2}\rho V_p^2 SbC_l \tag{3-25}$$

$$M_s = \frac{1}{2}\rho V_p^2 ScC_M \tag{3-26}$$

$$N_s = \frac{1}{2}\rho V_p^2 SbC_N \tag{3-27}$$

Where, $C_l, C_M\ and\ C_N$ are the aerodynamic coefficients, S is the wing area, b is the wing span length and c is the cord length of the wing. The coefficients are dependent of other state parameters like it is illustrated on the forces section.

$$C_l = C_{l_\beta}\beta + C_{l_p}\bar{p} + C_{l_r}\bar{r} + C_{l_{\delta_a}}\delta_a + C_{l_{\delta_r}}\delta_r \tag{3-28}$$

Where, δ_a is the aileron displacement which is one of the control surfaces along the x-axis.

$$\bar{p} = \frac{b}{2V_p}p_s\ ; p_s = pcos\alpha + rsin\alpha \tag{3-29}$$

$$\bar{r} = \frac{b}{2V_p}r_s\ ; r_s = -psin\alpha + rcos\alpha \tag{3-30}$$

$$C_M = C_{M_0} + C_{M_\alpha}\alpha + C_{M_{\delta_e}}\delta_e + C_{M_q}\bar{q} + C_{M_{\dot{\alpha}}}\dot{\alpha}' \tag{3-31}$$

Where, $\bar{q} = \frac{c}{2V_p}q, \qquad \dot{\alpha}' = \frac{c}{2V_p}\dot{\alpha}$

$$C_N = C_{N_\beta}\beta + C_{N_p}\bar{p} + C_{N_r}\bar{r} + C_{N_{\delta_a}}\delta_a + C_{N_{\delta_r}}\delta_r \tag{3-32}$$

3.5 Gravity Forces

On the atmospheric environmetn, gravitational forces are acting on the body with a representation of mg, where m is mass of the aircraft and g is the gravitational acceleration along the z_e axis. In order to represent the vector of gravitational forces on the body axes, the mathematical expression will be like below:

$$g_x = -mgsin\theta \tag{3-33}$$

$$g_y = mgcos\theta sin\Phi \tag{3-34}$$

$$g_z = mgcos\theta cos\Phi \tag{3-35}$$

3.6 Translational Equations in Wind Axes

In the Section 3.3, the translational equations of motion are represented in terms of body axes. As it is analyzed in the previous sections, aerodynamic forces and moments are dependent of V_p, α, β parameters. In order to get these parameters, wind axes expressions of the translational equations of motion has to be explained, clearly.

$$\overrightarrow{V_p} = V_p \overrightarrow{\imath_w} \tag{3-36}$$

$$\vec{\Omega} = p_w \overrightarrow{\imath_w} + q_w \overrightarrow{\jmath_w} + r_w \overrightarrow{k_w} \tag{3-37}$$

$$\frac{d\overrightarrow{V_p}}{dt}|i = \dot{V_p} \overrightarrow{\imath_w} + r_w V_p \overrightarrow{\jmath_w} - q_w V_p \overrightarrow{k_w} \tag{3-38}$$

Since the total forces are equalt to the equation (3-38), it can be represented as like below if the equations are rearrenged according to wind axes parameters:

$$\dot{V_p} = \frac{F_{wx}}{m} \tag{3-39}$$

$$\dot{\alpha} = \frac{\left(-p_s sin\beta + q cos\beta + \frac{F_{wz}}{mV_p}\right)}{cos\beta} \tag{3-40}$$

$$\dot{\beta} = r_w - r_s = r_w - (-p sin\alpha + r cos\alpha) \tag{3-41}$$

The parameters angle of attack and side-slip angle can be expressed in terms of linear velocities:

$$\alpha = \tan^{-1} \frac{w}{u} \tag{3-42}$$

$$\beta = \sin^{-1} \frac{v}{V_p} \tag{3-43}$$

Where, the velocity term V_p $can\ be\ represented\ as$

$$V_p = \sqrt{u^2 + v^2 + w^2} \tag{3-44}$$

4. FLIGHT CONTROL SYSTEM OF THE AIRCRAFT

By improvement of the technology, the aircrafts are developed in a very modern way. Especially, the fighter aircrafts are not easy to control by pilots. The reason of these conditions are the nonlinearity expressions, systems of the aircraft. For this reason, a control system had to be developed by means of controlling the aircrafts. These could be done via controlling following command of a ubsystem, engine or a control surface.

The flight envelope, flight path, velocity of the aircraft has to be also controlled. The control system can be implemented for several subsystem as it is explained above. It can be applied to control the velocity via engines by controlling the throttle. For this case, throttle become a control parameter which can maket he velocity of the aircraft in total.

The other and the most important subsystem is the control surfaces. They can be expressed like below in general:

Aileron : Controls the roll motion
Elevator: Controls the pitch motion
Rudder : Controls the yaw motion

In a result, when it is considered that the contents of the flight control system is a configuration of all these control elements which control the total forces and moments action on the aircraft. These are completed when the control surface and the effects of other elements are configured. The most important flight control principle are roll, pitch and yaw control. These controls are all dependent of the system parameters and control parameters.

Furthermore, the aircraft can be also affected by the enviromental conditions changes, even if the pilot system feeds the correct inputs. In order to overcome this issue, the control system plays a cruical role, when it is considered this subject.

In conclusion, when all of these operations and manipulations are considered as automatically, here might be a control system such that it can consider, configure and operate all of the conditions in a proper way. There are some techniques to do that. In this chapter, these techniques are explained briefly.

4.1. History of the Flight Control System

At the beginning of 20th century, the technology of the aircrafts were developed by aerospace industry. One of the majör improvement of these technology was the pilot-aircraft interface which leads to control the whole aircraft.

Firstly, which is very common example, Wright brothers developed was developed their systems. Fort he later years controlling the aircrafts became very hard, since the complexity of the system which is a nonlinear system and the defining the aerodynamical effects fort he aircraft.

Second big progress was the development of the wind tunnel. This makes the characteristics of the aircraft in terms of mathematical expression. This leads to explaining the aerodynamical coefficients. Thus, the effect of aerodynamic coefficients to the aircraft were began to consider and expressed mathematically. As a result of this, the flight path, flight envelope and maneuvering capability of the aircraft were be able to control manually for the first time easily. By the improvement of technology and the control methods, it became automatically. In conclusion, the history of the control system got a very long and full of experiences way.

4.2. Flight Control Methods

By improvement of the technology and the aircraft complexity, the classical control methods became not enough fort he system. This was because of the amount of the control parameters and increasing performance issue, most importantly. Therefore, control methods were developed in time dramatically. In this chapter, some of the important methods will be explained.

4.2.1 Nonlinear dynamic inversion control method

In general, linear control methods can not satisfy the specific conditions for the current aircraft flight envelope or maneuvre. The reason is that the states can change easily or the adaptivity of the control system can not catch the current state changes. In order to overcome this issue, nonlinear control methods were developed, since the aircraft Dynamics have highly nonlinear terms. Thus, the control system can easily adapt the state changes at each flight conditions or specified equilibrium states.

The developed control systems were designed to catch the derivation of the inputs, surface deflections and the nonlinear states so that the following control coefficients or functions or parameters of the controller can response the changes easily. According to these developments and the applications, adaptive control method was named which contains all of definitions and expressions. After all, there is also a common control method which was named as dynamic inversion control. This method also satisfies the explained situations. A further explanation of the dynamic inversion method within the nonlinearity conditions is defined as Nonlinear Dynamic Inversion. This method is explained in the next chapter.

Nonlinear Dynamic inversion control system is one of the common flight control method for the aircraft control systems. The principle depends on the feedback linearization (Albostan, 2017). Aircrafts have nonlinear behaviours in terms of the dynamics and motions. In the control systems, the structure has to be satisfy all of the nonlinear conditions without getting big amount of error so that th eaircraft can move on or flight within the specified path and envelope. Therefore, the control system contents have to be modelled mathematically. At the previous chapters, there were some methods which can overcome this subject. However, these operations were done by linearizing the whole system. Hence, the controller was also linear, since the controlled plant model was linearized.

In general, the main controller contains engine control throttle, control surface deflections and state feedbacks. Therefore, these parameters have to be modelled without any linearization methods so that they can feed back into controller inputs not by losing any characteristics in terms of dynamics. The main idea is the adaptivity of the control parameters in terms of nonlinearity. In this way, the robustness of the control system will be kept within the optimum conditions so that the performance will increase, eventually.

Since the aircraft control systems has cascaded structure mostly, the response of the specific subsystems can mismatch the state changes. Therefore, in this study, NDI control method is designed as two stage in order to feed the outputs to the corresponding inputs of the subsystems. For this reason, similarity of the NDI and the feedback linearization method are explained mostly.

The main principle is the making difference between reference inputs and feedback-states zero which means that the error will go to zero. By applying the method in this way, the inputs and corresponding outputs remain nonlinear. Since there is no linearization, the state-flow signals make their way with their original structure. The stages implemented to the NDI systems can be explained like below:

Slow-State Dynamic Control Loop: Derives the reference angular rates p_c, q_c, r_c according to the given wind axes reference inputs α_c, β_c, μ_c

Fast-State Dynamic Control Loop: Derives the reference control surface deflections $\delta_a, \delta_e, \delta_r$ according to the reference inputs which are coming from the slow-state dynamic control loop outputs.

The mathematical background of NDI control method is explained in the next chapter.

4.2.1.1 Mathematical definitions

Since NDI control method is similar to the feedback linearization as it was explained in the previous chapters, the mathematical expressions of this method can be represented like below:

$$\dot{X} = F(X) + G(X)u \tag{4-1}$$

$$y = h(x) \tag{4-2}$$

Where, X is the state vector of the controlled part of the aircraft dynamics, G is an mxm input matrix, *if it is not a square matrix, there will be a control allocation to make it inversible,* Y is the output of the controller and the H is nonlinear vector function.

$$u = \mathrm{G}^{-1}[\dot{\mathrm{X}}_{\mathrm{des}} - \mathrm{F(X)}] \tag{4-3}$$

U is the control vector of the controller. It is solved so that the input matrix and current states conditions will be satisfied for the case of adapting the stability. However, sometimes G matrix is not a square matrix.

In a further explanation, the structure of the control method will be like below:

$$\dot{y} = \frac{\delta h}{\delta x} F(x) + \frac{\delta h}{\delta x} G(x)u \tag{4-4}$$

Let,

$$A = \frac{\delta h}{\delta x} F(x) \tag{4-5}$$

$$B = \frac{\delta h}{\delta x} G(x) \tag{4-6}$$

$$u = A^{-1}[v - B] \tag{4-7}$$

Where, v is the pseudo control which is a virtual control. It is equal to the time derivative of the output vector

The block diagram of this operation is shown in figure Figure 4.1:

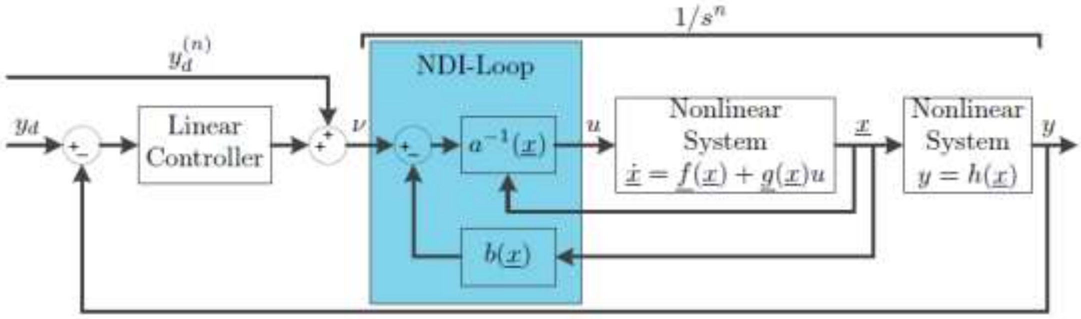

Figure 4.1 : Block diagram of NDI control loop

In Equation (4-7), A matrix is not a square matrix, always. In such cases, there has to be applied some control allocation in order to apply matrix inversion lemma. If it is considered a non-square and an optimization issue is wanted to implement, there will be a cost function which will derive a control output vector. Equation (4-8) shows the cost function.

$$J = \Delta u^T W \Delta u \tag{4-8}$$

$$\dot{y} = \dot{y_{des}} \tag{4-9}$$

$$\dot{y} = h_x(\dot{x_0} + A(x - x_0) + B_0 \Delta u) \tag{4-10}$$

$$\Delta u = W^{-1} B_h^T \left[B_h W^{-1} B_h^T\right]^{-1} \{\dot{y_{des}} - h_x[\dot{x_0} + A_0(x - x_0)]\} \tag{4-11}$$

Where B_h is expressed as $h_x B_0$ and B_0 is expressed as $\frac{\delta G}{\delta u}$ mathematically. W is the weighting matrix which is designed and choosed as a diagonal. The final control expression will be in equation (4-12) when the equation zz is rearrenged.

$$\Delta u = W^{-1} B_h^T \left[B_h W^{-1} B_h^T\right]^{-1} (\dot{y_{des}} - h_x \dot{x_0}) \tag{4-12}$$

$$\Delta u = u_c - u_0 \tag{4-13}$$

From the equation (4-8) to (4-13), the matrix inverse lemma of A is solved. By this case, the optimum solution for the control vector u is also solved for the specified or reference input states.

4.2.1.2 Designing the control law

In previous chapter, general definition of NDI control method was explained briefly. In this chapter, the control law is applied to the aircraft. The controller consists of two state; the first one is the slow-state control loop which is fed with wind-axes reference inputs and derives the corresponding outputs, and the second one is the fast-state control loop which is fed from the outputs of the first state as a reference inputs.

The first thing to design the control law for aircraft is that defining the state equations for the controller part.

$$\dot{V_p} = \frac{1}{m}(-Z_s + Tcos\alpha cos\beta) - gsin\gamma \tag{4-13}$$

$$\dot{\alpha} = q - tan\beta(pcos\alpha + rsin\alpha) - \frac{1}{mV_p cos\beta}(Z_s + Tsin\alpha) + \frac{gcos\gamma cos\mu}{V_p cos\beta} \tag{4-14}$$

$$\dot{\beta} = -rcos\alpha + psin\alpha + \frac{1}{mV_p}(Y_s - Tcos\alpha sin\beta) + \frac{gcos\gamma sin\mu}{V_p} \tag{4-15}$$

$$\dot{\gamma} = \frac{1}{mV_p}\big(Z_s cos\mu - Y_s sin\mu + T(cos\alpha sin\beta sin\mu + sin\alpha cos\mu)\big) - \frac{gcos\gamma}{V_p} \tag{4-16}$$

$$\dot{\mu} = \frac{pcos\alpha + rsin\beta}{cos\beta} + \frac{1}{mV_p}\big(Y_s cos\mu tan\gamma + Z_s(sin\mu tan\gamma + tan\beta) + T(sin\alpha tan\gamma sin\mu + sin\alpha tan\beta - cos\alpha tan\gamma cos\mu sin\beta)\big) - \frac{gcos\gamma cos\mu tan\beta}{V_p} \tag{4-17}$$

$$\dot{\chi} = \frac{1}{mV_p\gamma}(Z_s sin\mu + Y_s cos\mu + T(sin\alpha sin\mu - cos\alpha sin\beta cos\mu)) \tag{4-18}$$

$$\dot{p} = a_1 rq + a_2 pq + a_3 L_x + a_4 N_x \tag{4-19}$$

$$\dot{q} = a_5 pr - a_6 p^2 + a_6 r^2 + a_7 M_x \tag{4-20}$$

$$\dot{r} = a_8 pq - a_2 rq + a_4 L_x + a_9 N_x \tag{4-21}$$

4.2.1.3 Slow-state control loop

Slow-State control loop is designed as taking reference input as wind-axes parameters which are α, β, μ, the following reference outputs p_c, q_c and r_c are inverted by feeding back the dynamic states. The mathematical expressions are defined below:

$$\begin{bmatrix} \dot{\alpha_c} \\ \dot{\beta_c} \\ \dot{\mu_c} \end{bmatrix} = \begin{bmatrix} \dot{\alpha} \\ \dot{\beta} \\ \dot{\mu} \end{bmatrix}_{from\ the\ state\ feedback} \Longrightarrow \begin{bmatrix} p_c \\ q_c \\ r_c \end{bmatrix} \text{ Slow-State Dynamic Control Loop}$$

The terms $\dot{\alpha_c}, \dot{\beta_c}$ and $\dot{\mu_c}$ are generated as gaining from angular proportional gains, w_α, w_β and w_μ . The matrix shown below is the weighting matrix, $W_{1_{\alpha\beta\mu}}$, which consists of these proportional gains. The values of these gains for this loop are generally between 1~2 rad/s.

$$\begin{bmatrix} \dot{\alpha_c} \\ \dot{\beta_c} \\ \dot{\mu_c} \end{bmatrix} = W_{1_{\alpha\beta\mu}} \begin{bmatrix} \alpha_c \\ \beta_c \\ \mu_c \end{bmatrix} = \begin{bmatrix} w_\alpha & a_{12} & a_{13} \\ a_{12} & w_\beta & a_{23} \\ a_{13} & a_{23} & w_\mu \end{bmatrix} * \begin{bmatrix} \alpha_c \\ \beta_c \\ \mu_c \end{bmatrix} \tag{4-22}$$

Where, a_{12}, a_{13}, a_{23} are off-diagonal weighting matrix terms which are generally set to zero.

$$\begin{bmatrix} \dot{\alpha_c} \\ \dot{\beta_c} \\ \dot{\mu_c} \end{bmatrix} = \left(\begin{bmatrix} g_\alpha \\ g_\beta \\ g_\mu \end{bmatrix} + \begin{bmatrix} -tan\beta * cos\alpha & 1 & -tan\beta * sin\alpha \\ sin\alpha & 0 & -cos\alpha \\ cos\alpha/cos\beta & 0 & sin\alpha/cos\beta \end{bmatrix} * \begin{bmatrix} p \\ q \\ r \end{bmatrix} \right) \tag{4-23}$$

Where,

$$g_\alpha = \frac{1}{V_p * cos\beta} * (-A_x * sin\alpha + A_z * cos\alpha + g * \cos\gamma * cos\mu) \tag{4-24}$$

$$g_\beta = -sin\beta * \frac{A_x * cos\alpha + A_z * sin\alpha}{V_p} + g * \cos\gamma * \frac{cos\mu}{V_p} \tag{4-25}$$

$$g_\mu = A_y * cos\beta * cos\mu * \frac{tan\gamma}{V_p} + (A_x * sin\alpha - A_z * cos\alpha) * \frac{\tan\gamma * sin\mu + tan\beta}{V_p} - (A_x * cos\alpha + A_z * sin\alpha) * \frac{tan\gamma * cos\mu * sin\beta}{V_p} - g * cos\gamma * cos\mu * \frac{tan\beta}{V_p} \tag{4-26}$$

A_x, A_y *and* A_z are the normal accelerations which are transform from the wind axis aerodynamic force equatins and body axis force equations. The Equations (4-24), (4-25) and (4-26) are generated from the state equations from the beginning of this chapter. In conclusion, according to equation (4-23), the expressions above can be inverted as the NDI control method so that the desired outputs can generate.

$$\begin{bmatrix} p_c \\ q_c \\ r_c \end{bmatrix} = \begin{bmatrix} -tan\beta * cos\alpha & 1 & -tan\beta * sin\alpha \\ sin\alpha & 0 & -cos\alpha \\ cos\alpha/cos\beta & 0 & sin\alpha/cos\beta \end{bmatrix}^{-1} \left(\begin{bmatrix} \dot{\alpha}_c \\ \dot{\beta}_c \\ \dot{\mu}_c \end{bmatrix} - \begin{bmatrix} g_\alpha \\ g_\beta \\ g_\mu \end{bmatrix} \right) \qquad (4\text{-}27)$$

The block diagram of the slow-state control loop is shown in Figure 4.2 in terms of mathematical expression of MATLAB/Simulink program:

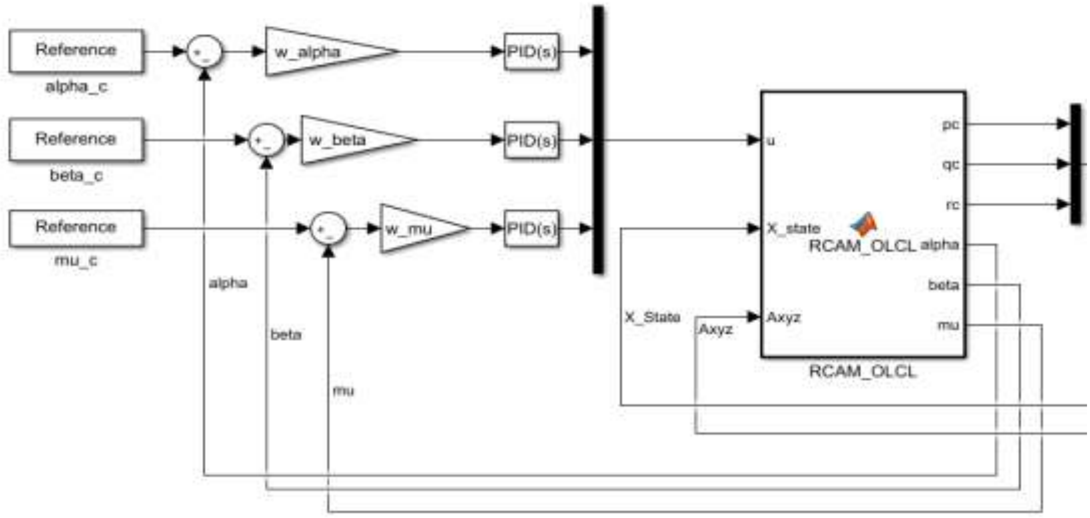

Figure 4.2 : Slow-state control loop diagram

4.2.1.4 Fast-state control loop

Fast-State Control Loop is designed as inputs and inverted following outputs. The inputs of this state are generated from the slow-state control loop as reference, p_c, q_c *and* r_c. In this control loop, there are aerodynamic Dynamics of the aircraft. Therefore, the aerodynamic forces and moments are mostly dealt with. The following output which is set of control surface deflections, δ_a, δ_e *and* δ_r are generated from the state equations of aerodynamic forces and moments. These control surfaces are corresponding to the general output of the controller so that they can be assumed as output state vector, y.

$$\begin{bmatrix} \dot{p_c} \\ \dot{q_c} \\ \dot{r_c} \end{bmatrix} = \begin{bmatrix} \dot{p} \\ \dot{q} \\ \dot{r} \end{bmatrix}_{from\ the\ state\ feedback} \Longrightarrow \begin{bmatrix} \dot{\delta_a} \\ \dot{\delta_e} \\ \dot{\delta_r} \end{bmatrix} \text{ Fast-State Dynamic Control Loop}$$

The terms $\dot{p_c}, \dot{q_c}\ and\ \dot{r_c}$ are generated as gaining from angular proportional gains, $w_p, w_q\ and\ w_r$. The matrix shown below is the weighting matrix, $W_{1_{pqr}}$, which consists of these proportional gains. The values of these gains for this loop are generally between 3~5 rad/s.

$$\begin{bmatrix} \dot{p_c} \\ \dot{q_c} \\ \dot{r_c} \end{bmatrix} = W_{1_{pqr}} \begin{bmatrix} p_c \\ q_c \\ r_c \end{bmatrix} = \begin{bmatrix} w_p & a_{12} & a_{13} \\ a_{12} & w_q & a_{23} \\ a_{13} & a_{23} & w_r \end{bmatrix} \begin{bmatrix} p_c \\ q_c \\ r_c \end{bmatrix} \tag{4-28}$$

Where, a_{12}, a_{13}, a_{23} are off-diagonal of the weighting matrix terms, which are generally set to zero.

$$\begin{bmatrix} \dot{p_c} \\ \dot{q_c} \\ \dot{r_c} \end{bmatrix} = \left(\begin{bmatrix} g_p \\ g_q \\ g_r \end{bmatrix} + \begin{bmatrix} F_{p_{\delta_a}} & 0 & F_{p_{\delta_r}} \\ 0 & F_{q_{\delta_e}} & 0 \\ F_{r_{\delta_a}} & 0 & F_{r_{\delta_r}} \end{bmatrix} * \begin{bmatrix} \delta_a \\ \delta_e \\ \delta_r \end{bmatrix} \right) \tag{4-29}$$

Where,

$$g_p = \frac{(I_z*LL+I_{xz}*NN)}{I_x*I_z-I_{xz}^2} + \frac{(I_{xz}*(I_x-I_y+I_z)*p*q+(I_z*(I_y-I_z)-I_{xz}^2)*q*r)}{I_x*I_z-I_{xz}^2} \tag{4-30}$$

$$g_q = \frac{MM}{I_y} + \frac{(I_z-I_x)*p*r+I_{xz}*(r^2-p^2)}{I_y} \tag{4-31}$$

$$g_r = \frac{I_{xz}*LL+I_x*NN}{I_x*I_z-I_{xz}^2} + \frac{(I_x*(I_x-I_y)-I_{xz}^2)*p*q-I_{xz}(I_x-I_y)*q*r}{I_x*I_z-I_{xz}^2} \tag{4-32}$$

$$F_{p_{\delta_a}} = \frac{(I_{xz}C_{l_{\delta a}}+I_xC_{N_{\delta a}})}{I_xI_z-I_{xz}^2} \tag{4-33}$$

$$F_{p_{\delta_r}} = \frac{(I_{xz}C_{l_{\delta r}}+I_xC_{N_{\delta r}})}{I_xI_z-I_{xz}^2} \tag{4-34}$$

$$F_{q_{\delta_e}} = \frac{C_{M_{\delta e}}}{I_y} \tag{4-35}$$

$$F_{r_{\delta_a}} = \frac{(I_z C_{l_{\delta a}} + I_{xz} C_{N_{\delta a}})}{I_x I_z - I_{xz}^2} \tag{4-36}$$

$$F_{r_{\delta_r}} = \frac{(I_z C_{l_{\delta r}} + I_{xz} C_{N_{\delta r}})}{I_x I_z - I_{xz}^2} \tag{4-37}$$

The Equations from (4-33) to (4-37) are the mass moment of inertia terms. The mathematical expressions above can be inverted in order to form as the fast-state control loop structure. Hence, the corresponding outputs $\delta_a, \delta_e\ and\ \delta_r$ can be fed to the aircraft Dynamics state subsystem so that the whole model can operate in an order. The block diagram of the fast-state control loop is shown in Figure 4.3.

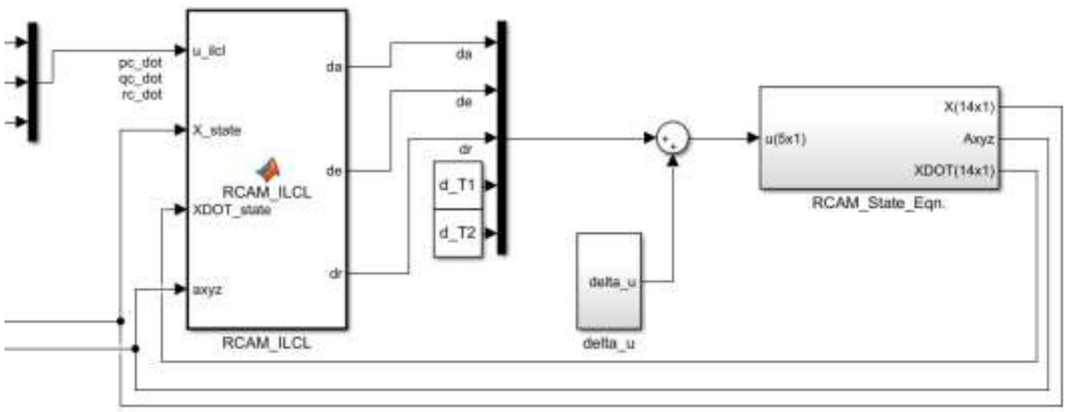

Figure 4.3 : Fast-state control loop

4.2.2 Linear flight control methods

Linearization is applied to the airframe model of the aircraft by using Taylor Series expansion method.

$$f(x,y,z,\dots) = f(x_0,y_0,z_0,\dots) + \left(\frac{\partial f}{\partial x}\right)_{x=x_0}(x-x_0) + \left(\frac{\partial f}{\partial y}\right)_{y=y_0}(y-y_0) + \left(\frac{\partial f}{\partial z}\right)_{z=z_0}(z-z_0) + \cdots \quad \text{(neglected high-order terms)} \tag{4-38}$$

$$f(x,y,z,\dots) = f(x_0,y_0,z_0,\dots) + \left(\frac{\partial f}{\partial x}\right)_{x=x_0}\delta x + \left(\frac{\partial f}{\partial y}\right)_{y=y_0}\delta y + \left(\frac{\partial f}{\partial z}\right)_{z=z_0}\delta z + \cdots \tag{4-39}$$

4.2.2.1 Linearization of longitudinal equations

Since this study deals with the longitudinal motion control issue, the linearization consists of the longitudinal motion state equations of motions. Therefore, the desired and referenced or operating condition points are considered and applied to the model with linearization. The trim conditions are applied to the longitudinal motion in order to obtain linearized state-space equations. All the trim conditions are listed as follow:

Trim Conditions:

$$\left.\begin{aligned} &\beta(t) = 0 \\ &p(t) = 0 \\ &r(t) = 0 \\ &\Phi(t) = 0 \\ &\mathrm{V_p}(t) = \mathrm{V_{p_0}} = \mathrm{constant} \\ &\alpha(t) = \alpha_0 = constant \\ &q(t) = q_0 = 0 \\ &\theta(t) = \theta_0 = constant \end{aligned}\right\} \tag{4-40}$$

In this aircraft model, which is hypotetical supersonic aircraft, the level flight conditions are calculated as the angle of attach value has to be zero. Therefore, in Equation (4-40) , the value is assumed as $\boldsymbol{\alpha_0 = 0}$. Hence, the derivation of the linearized longitudinal motion state equations can be simplified further like below:

$$V_p = V_{p_0} + \delta v_p \tag{4-41}$$

$$\alpha = \alpha_0 + \delta\alpha; \tag{4-42}$$

$$q = q_0 + \delta q; \tag{4-43}$$

$$\theta = \theta_0 + \delta\theta; \tag{4-44}$$

According to the assumptions and the conditions in Equations from (4-41) to (4-44) , the above equations can be written as below for the sake of simplification:

$$V_p = V_{p_0} + \delta v_p \tag{4-45}$$

$$\alpha = \delta\alpha \tag{4-46}$$

$$q = \delta q \tag{4-47}$$

$$\theta = \delta\theta \tag{4-48}$$

The nonlinear version of the longitudinal motion equations are expressed in Equations (4-49) and (4-50). The velocity term, V_p and α, are expressed below according to above equations:

$$\dot{V_p} = \sum \frac{F_{x_W}}{m} = \frac{F_D + P_{x_S} + G_{x_S}}{m} \tag{4-49}$$

$$\dot{\alpha} = q + \sum \frac{F_{z_W}}{m} = \frac{F_L + P_{z_S} + G_{z_S}}{m} \tag{4-50}$$

And the pitching motion terms, q and θ, are expressed below like above equations:

$$\dot{q} = \frac{MM}{I_{yy}} \tag{4-51}$$

$$\dot{\theta} = q \tag{4-52}$$

These nonlinear equations are ready to be linearized via Taylor Series expansion. The first thing is that considering the initial states and the trim conditions. So that, Equations (4-49) and (4-50) are linearized like below in order to get the perturbation expressions. Before starting to the linearization, when the equations are put in according to the equation (4-45), the result can be seen below:

$$\dot{V_p} = \frac{-0.5\rho\left(V_{p_0} + \delta V_p\right)^2 S}{m}\left(C_{D_0} + C_{D_{CL^2}} C_L^2\right) + \frac{(P_x - mgsin\theta)cos\alpha + (P_z + mgcos\theta)sin\alpha}{m} \tag{4-53}$$

When the same operations are applied for angle of attack and the pitch rate, the expressions can be seen below:

$$\dot{\alpha} = q + \frac{-0.5\rho(V_{p_0}+\delta v_p)^2 S}{m}\left(C_{L_0} + C_{L_\alpha}\delta\alpha + C_{L_{\delta e}}\delta e\right) + \frac{g}{V_{p_0}+\delta v_p} - \frac{P_x\delta\alpha}{m(V_{p_0}+\delta v_p)} + P_z/m(V_{p_0} + \delta v_p) \qquad (4\text{-}54)$$

$$\dot{q} = \frac{0.5\rho(V_{p_0}+\delta v_p)^2 Sc}{I_{yy}}\left(C_{M_0} + C_{M_\alpha}\alpha + C_{M_{\delta_e}}\delta_e\right) + \frac{0.5\rho(V_{p_0}+\delta v_p)Sc}{2I_{yy}}\left(C_{M_q}q + C_{M_{\dot{\alpha}}}\dot{\alpha}\right) + \frac{T_y}{Iyy} \qquad (4\text{-}55)$$

$$\dot{\theta} = \delta q \qquad (4\text{-}56)$$

If the expressions like $cos\alpha\ and\ cos\theta \cong\ 1,\ \ sin\alpha\ and\ sin\theta \cong\ \alpha$are considered as these values the Equation (4-53) can be extracted by using Taylor Series expansion like below:

$$\delta\dot{v}_p = \frac{-0.5\rho V_{p_0}^2 S}{m}\left(C_{D_0} + C_{D_{CL^2}}C_{L_0}^2\right) + \frac{-0.5\rho V_{p_0}^2 S}{m}\left(2C_{D_{CL^2}}C_{L_0}C_{L_\alpha}\right)\delta\alpha +$$
$$\frac{-0.5\rho V_{p_0} S}{m}2\left(C_{D_0} + C_{D_{CL^2}}C_{L_0}^2\right)\delta v_p - g(\delta\theta - \delta\alpha) + \frac{P_x}{m} + \frac{P_z}{m}\delta\alpha \qquad (4\text{-}57)$$

In Equation (4-54) can be also extracted like above:

$$\delta\dot{\alpha} = \delta q + \frac{-0.5\rho V_{p_0} SC_{L_0}}{m} + \frac{-0.5\rho SC_{L_0}}{m}\delta v_p + \frac{-0.5\rho V_{p_0} SC_{L_\alpha}}{m}\delta\alpha + \frac{-0.5\rho V_{p_0} SC_{L_{\delta e}}}{m}\delta e + \frac{g}{V_{p_0}} -$$
$$\frac{g}{V_{p_0}^2}\delta v_p - \frac{P_x}{mV_{p_0}}\delta\alpha + \frac{P_z}{mV_{p_0}} - \frac{P_z}{mV_{p_0}^2}\delta v_p \qquad (4\text{-}58)$$

The Equations (4-57) and (4-58) can be simplified since the aircraft is desired to be in level flight. In this form, $\delta_e = 0$. Hence, the Equations (4-57) and (4-58 can be expressed with the following assumptions:

$$\frac{\rho V_{p_0}^2 S}{2}\left(C_{D_0} + C_{D_{CL^2}}C_{L_0}^2\right) + P_x = 0$$
$$\frac{\rho V_{p_0}^2 S}{2}C_{L_0} = mg + P_z\ \ (There\ is\ no\ propulsion\ force\ in\ z-direction, P_z = 0)$$

The new expression of the lift and drag coefficient can be derived by considering the expressions above:

$\widetilde{C_L} = C_{L_0}$
$\widetilde{C_D} = \left(C_{D_0} + C_{D_{CL^2}} C_{L_0}^2\right)$

For the pitching motion, pitch rate expression in Equation (4-55), is linearized below:

$$\dot{\delta q} = \frac{0.5\rho(V_{p_0})^2 Sc}{I_{yy}} C_{M_0} + \frac{0.5\rho V_{p_0} Sc}{I_{yy}} 2C_{M_0}\delta v_p + \frac{0.5\rho(V_{p_0})^2 Sc}{I_{yy}} C_{M_\alpha}\delta\alpha + \frac{0.5\rho(V_{p_0})^2 Sc}{I_{yy}} C_{M_{\delta e}}\delta e + \frac{0.5\rho(V_{p_0})^2 Sc^2}{I_{yy}} C_{M_q}\delta q + \frac{0.5\rho(V_{p_0})^2 Sc^2}{I_{yy}} C_{M_{\dot{\alpha}}}\dot{\delta a} + \frac{T_y}{I_{yy}} \quad (4\text{-}59)$$

Finally, the total linearized longitudinal motion state equations can be written like below in general form:

$$\dot{\delta v_p} = a_{11}\delta v_p + a_{12}\delta\alpha - a_{14}\delta\theta \quad (4\text{-}60)$$

$$\dot{\delta\alpha} = a_{21}\delta v_p + a_{22}\delta\alpha + a_{23}\delta q + b_2\delta e \quad (4\text{-}61)$$

$$\dot{\delta q} = a_{31}\delta v_p + a_{32}\delta\alpha + a_{33}\delta q - c_{32}\dot{\delta\alpha} + b_3\delta e \quad (4\text{-}62)$$

$$\dot{\delta\theta} = \delta q \quad (4\text{-}63)$$

These coefficients are expressed in Table 4.1 below:

Table 4.1. State-space form coefficients

$a_{11} = -\frac{2g\widetilde{C_D}}{V_{p_0} C_L'}$,	$a_{12} = -g(1 - 2C_{D_{C_L^2}} C_{L_\alpha})$,	$a_{14} = -g$
$a_{21} = -\frac{2g}{V_{p_0}^2}$,	$a_{22} = -\frac{g}{V_{p_0}}[\frac{C_{L\alpha}}{\widetilde{C_L}} + \frac{\widetilde{C_D}}{\widetilde{C_L}}]$,	$a_{23} = 1$
$a_{31} = 0$,	$a_{32} = \dfrac{mgcC_{M_\alpha}}{I_{yy}\widetilde{C_L}}$,	$a_{33} = \dfrac{mgc^2 C_{M_q}}{2I_{yy}V_{p_0}\widetilde{C_L}}$
$b_2 = \dfrac{-gC_{L_{\delta e}}}{V_{p_0}\widetilde{C_L}}$,	$b_3 = \dfrac{mgcC_{M_{\delta e}}}{I_{yy}\widetilde{C_L}}$,	$c_{23} = \dfrac{-mgc^2 C_{M_{\dot{\alpha}}}}{2I_{yy}V_{p_0}\widetilde{C_L}}$

The general matrix form is like below:

$$C\dot{X} = \mathrm{AX} + \mathrm{Bu} \tag{4-64}$$

Where,

$$C = \begin{bmatrix} 1 & 0 & 0 & 0 \\ 0 & c_{23} & 0 & 0 \\ 0 & 0 & 1 & 0 \\ 0 & 0 & 0 & 1 \end{bmatrix}, A = \begin{bmatrix} a_{11} & a_{12} & 0 & a_{14} \\ a_{21} & a_{22} & a_{23} & 0 \\ a_{31} & a_{32} & a_{33} & 0 \\ 0 & 0 & 1 & 0 \end{bmatrix}, B = \begin{bmatrix} 0 \\ b_2 \\ b_3 \\ 0 \end{bmatrix}, B = \begin{bmatrix} \delta v_p \\ \delta\alpha \\ \delta q \\ \delta\theta \end{bmatrix} \text{ and}$$

$u = \delta_e$

4.2.2.2 Building linearized airframe model

In previous chapter, the longitudinal state equations are linearized. So that, the airframe model can be developed in order to design a controller for the system. The matrix form in the previous chapter can be built in MATLAB/Simulink program to get an airframe model in Figure 4.4.

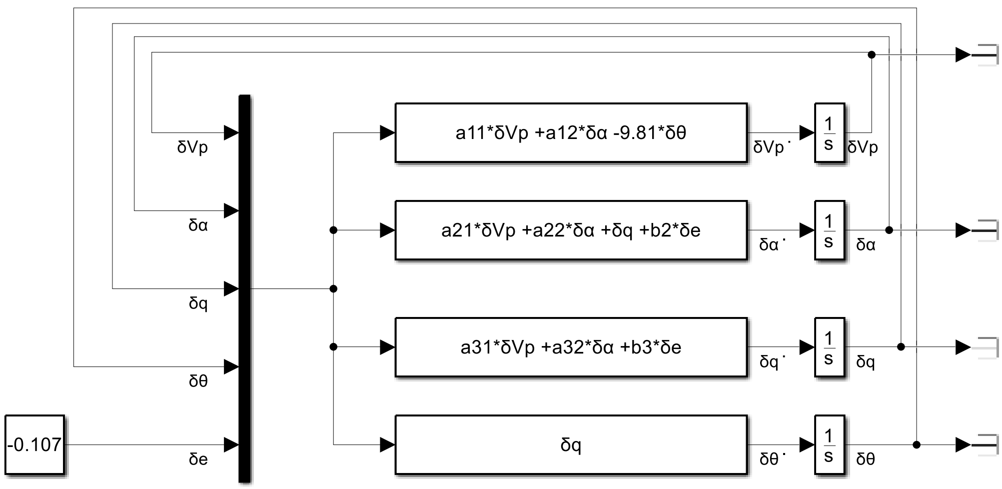

Figure 4.4 : Linearized Airfram Model (Longitudinal Motion)

Since this study deals with the longitudinal motion, the pitch angle θ behaviour with respect to the elevator displacement δe is important to analyze. Therefore, the linearized equation of these two expression can be converted to the transfer function like below:

$$\frac{Y_{\theta\delta e}(s)}{\delta e(s)} = \frac{(b_3-c_{32}b_2)s^2+[b_2(c_{32}a_{11}+a_{32})-b_3(a_{11}+a_{22})]s+b_3(a_{11}a_{22}-a_{21}a_{12})-b_2a_{32}a_{11}}{Den(s)} \quad (4\text{-}65)$$

Where,

$Den(s) = s^4 + (c_{32} - a_{11} - a_{22} - a_{33})s^3 + [a_{11}a_{22} - a_{21}a_{12} + a_{33}(a_{11} + a_{22}) - c_{32}a_{11} - a_{32}]s^2 + [c_{32}a_{21}a_{14} + a_{32}a_{11} - a_{33}(a_{11}a_{22} - a_{21}a_{12})]s + a_{32}a_{21}a_{14}$

When the pitching motion analyzed, it can be divided into two sections which are short-period and phugoid motion. At first, it is better to guarantee the stability for short-period apporximation, since the roots of the transfer operators are closer to the imaginary axis (border of the unstable region). If the stability is guaranteed in this motion period, the other periods can follow the reference commands in a stable way. The other reason of using the short-period appoximation at first is that the derivation of the velocity does not affect the angle of attack. Therefore, the designing of the controller can be studied with different velocity regims.

$$\frac{Y_{\theta\delta e}(s)}{\delta e(s)} = \frac{\left(\frac{b_3-b_2c_{32}}{a_{22}a_{33}-a_{32}}\right)s+\left(\frac{b_2a_{32}-b_3a_{22}}{a_{22}a_{33}-a_{32}}\right)}{s\left[\left(\frac{1}{a_{22}a_{33}-a_{32}}\right)s^2+\left(\frac{c_{32}-a_{33}-a_{22}}{a_{22}a_{33}-a_{32}}\right)s+1\right]} \quad (4\text{-}66)$$

$$\frac{Y_{\theta\delta e}(s)}{\delta e(s)} = \frac{-0.7206s-0.5144}{0.03087s^3+0.08553s^2+s} \quad (4\text{-}67)$$

4.2.2.3 Open-loop response of linearized airframe

The characteristic equation of the Equation (4-67) has to be analyzed for the static stability in order to decide and understand whether the aircraft is stable in level flight or not. Root Locus method is used for analyzing the static stability. The Figure 4.8 shows the expression beyond the pole and zero branches of the pitching motion of the linearized aircraft airframe. The result for the pithcing angle by feeding a small elevator discplacement motion can be seen in Figure 4.5:

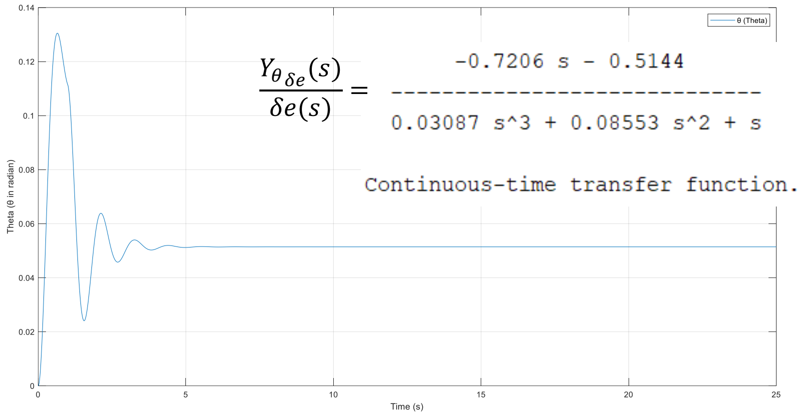

Figure 4.5 : Time response of pitching angle and elevator displacement

4.2.2.4 Open-loop response of linearized airframe with servo dynamic

The further dynamic which will be applied to the inner loop pitching motion is the elevator servo dynamics. This dynamic leads to the system in a more reality analysis. The common servo dynamic in terms of transfer function expression is like below:

$$Y_{elevator}(s) = -\frac{10}{s+10} \tag{4-68}$$

When the Equations (4-67) and (4-68) are considered as the inner loop plant transfer operator, it is better to analyze the static stability by producting of these two equation, since they can be considered as a combined open-loop transfer function like in Figure 4.6.

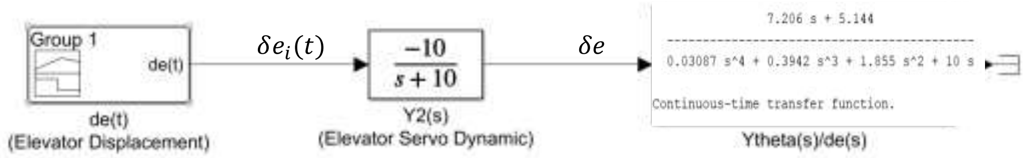

Figure 4.6 : Block diagram of short-period approximation with elevator servo dynamic

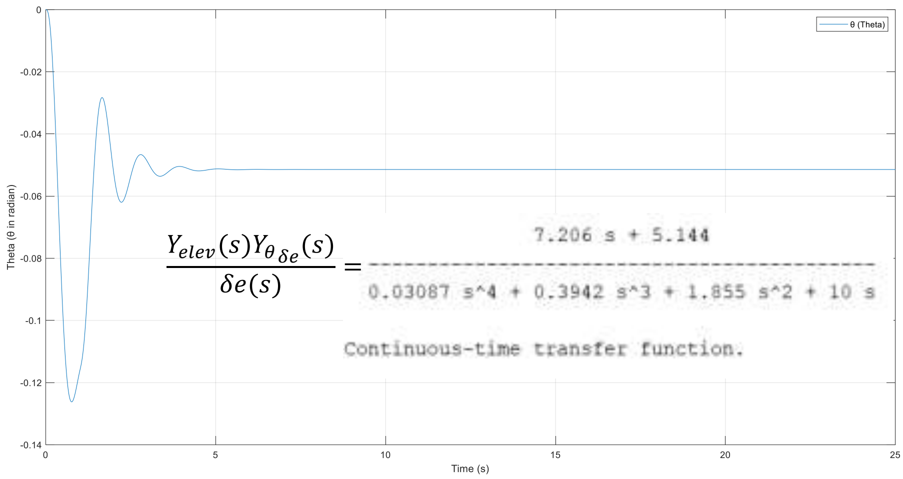

Figure 4.7 : Time response of pitching angle with respect to elevator displacement including elevator servo dynamic

According to the Figure 4.7, the system more stable if it is compared with the Figure 4.5. The way which has to be followed should be changing the servo, so that the dynamic of this equipment is also changed, in order to get the pitching angle following the reference pitching angle.

Since, the open-loop responses are studied, the control method can be chosen to design a suitable and optimum controller. There are several linear control methods such as Routh-Hurwitz Criteria, P.I.D controller, Root-Locus control method. In this study, Root-Locus control method is chosen because of the represantation of changing the parameters better than the other techniques. In the next chapter, the Root-Locus control method is implemented to the linearized airframe model.

4.2.2.6 Implemention of Root-Locus method

Since the open-loop responses are studied, the controller design should be applied to the airframe. Before considering the servo dynamic effect to the airframe, the short-period approximation characteristic can be seen below in Figure 4.8:

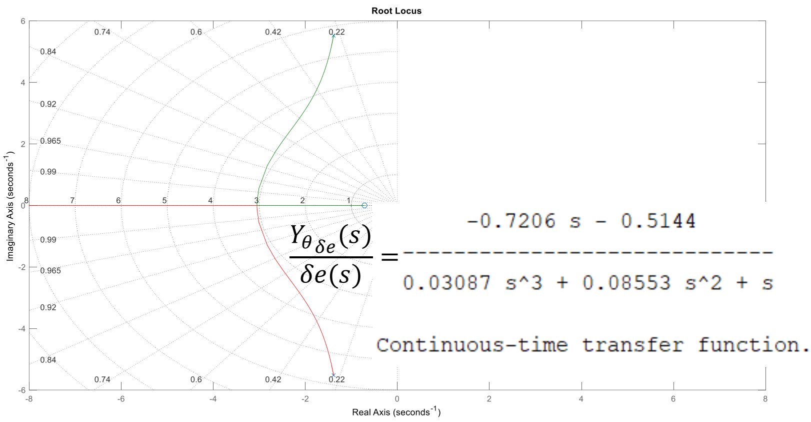

Figure 4.8 : Root-Locus diagram of short-period approximation

Since the dynamic of the servo actuators affect directly to the airframe in real, the system behaves more realistic. Therefore, choosing the right servos are getting important. The reason of that, choosing servo actuators affects the dynamic stability. It can be seen in Figure 4.9:

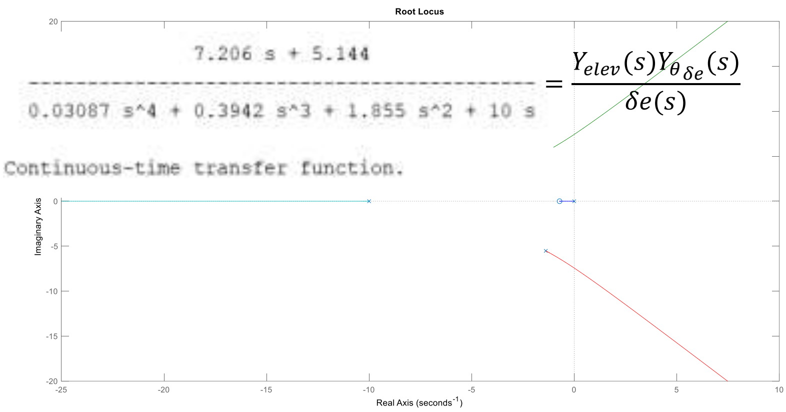

Figure 4.9 : Root-Locus diagram of short-period approximation with servo Dynamics

4.2.2.7 Inner loop controller

In order to get a closed-closed loop controller which is feeding the outer controller, the controller design is implemented to the airframe.

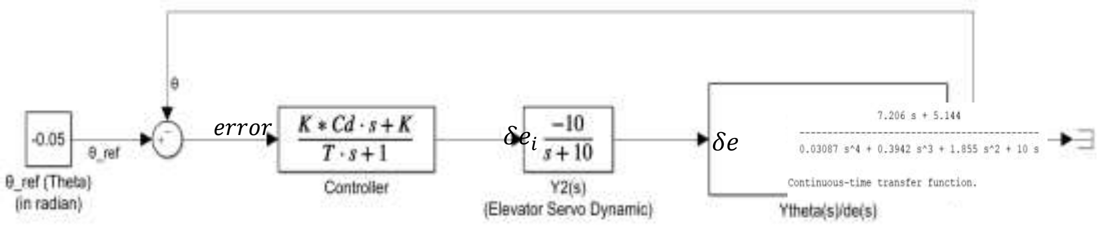

Figure 4.10 : Block diagram of inner control loop

When the Figure 4.10 is analyzed, the place of the controller coefficients can be estimated roughly in Root-Locus diagram. In order to get an optimum solution, the other control methods can be used, too. However, in this controller design, the coefficients can be estimated like below:

$$C(s) = \frac{K(C_d s+1)}{\tau s+1} \tag{4-69}$$

Inserted pole to the airframe is : $s = -1/\tau$

Inserted zero to the airframe is : $s = -1/C_d$

When the inserted pole and zeros are placed into the Root-Locus diagram, the approximate control can be applied to the inner loop. In Figure 4.11, the point A can be chose as an inserted additional zero-branch position for the airframe within the scope of $s = -\frac{1}{C_d}$.

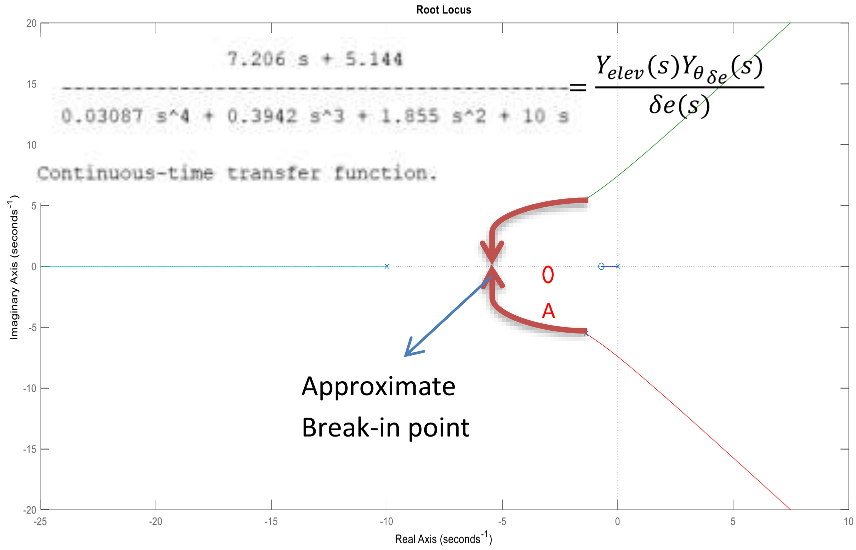

Figure 4.11 : Root-Locus diagram of inner loop controller (zero)

The inserted pole branch is placed a little far away from the pole at negative side, which is shown in Figure 4.12 with red star. In this case, the integrated pole goes to negative infinity asymptote, and the conjugate pole pair can be forced to diverge from the imaginary axis which is unstable region critical area. So that, two pole branches go to the other asymptotes by staying at the negative side of the Root-Locus diagram. This leads to the system for choosing controller gain without any doubt in terms of stability. The expression of this manipulation is explained graphically below:

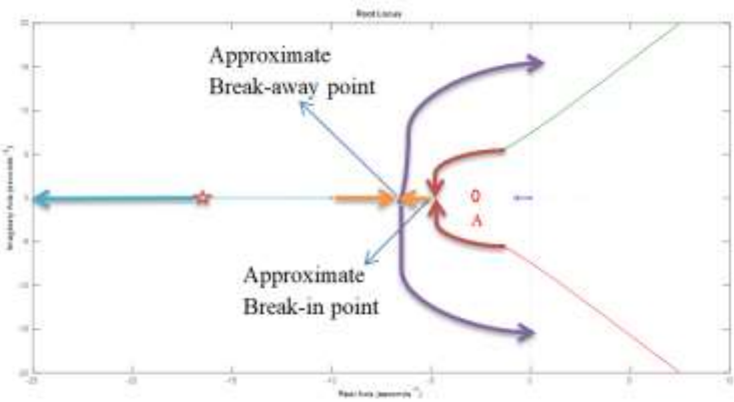

Figure 4.12 : Root-Locus diagram of inner loop controller (pole-zero)

The approximate places of the inserted pole and zero branches are shown at Figure 4.12. The remain proportional constant can be chose from the lines which are going to the asymptotes, freely in every bound, since the system is stable for each condition of this flight regime. A rough controller design can be analyzed in this way. However, in order to choose a proper and optimum solution for the inner loop. The total closed-loop transfer function is expressed below:

$$G_{inner}(s) = C(s)Y_2(s)Y_{\theta_{\delta e}}(s) = \frac{K(C_d s+1)(7.206s+5.144)}{(\tau s+1)(0.03087s^4+0.3942s^3+1.855s^2+10s)} \tag{4-70}$$

Implementing the reasonable pole and zero branch positions for the above closed-loop transfer function, $G_{inner}(s)$, the following controller constants can be established:

$\tau \ = 0.05$
$C_d = 0.2$

Above results for the controller coefficients leads to the total system in Root-Locus diagram like below in Figure 4.13:

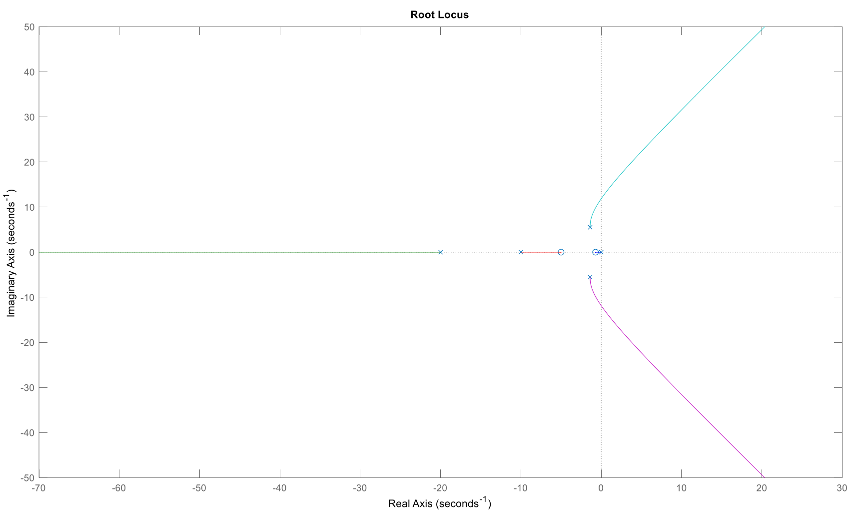

Figure 4.13 : Root-Locus diagram of inner loop controller (desired)

The Root-Locus diagram in Figure 4.13, is not comparable with the desired one at Figure 4.12. This is not a reliable solution for this plant, because the system can behaves unstable motion at some trim and reference conditions. Therefore, the conjugate pole pairs can be forced to the negative right hand side (stable region) by one more inserting same additional pole and zero branches. This leads the systems to an expression like in Equation (4-71):

$$G_{inner}(s) = C(s)Y_2(s)Y_{\theta_{\delta e}}(s) = \frac{K(C_d s+1)^2(7.206s+5.144)}{(\tau s+1)^2(0.03087s^4+0.3942s^3+1.855s^2+10s)} \tag{4-71}$$

In above equation, the characteristic of the open-loop transfer function is expressed in Figure 4.14 with Root-Locus diagram:

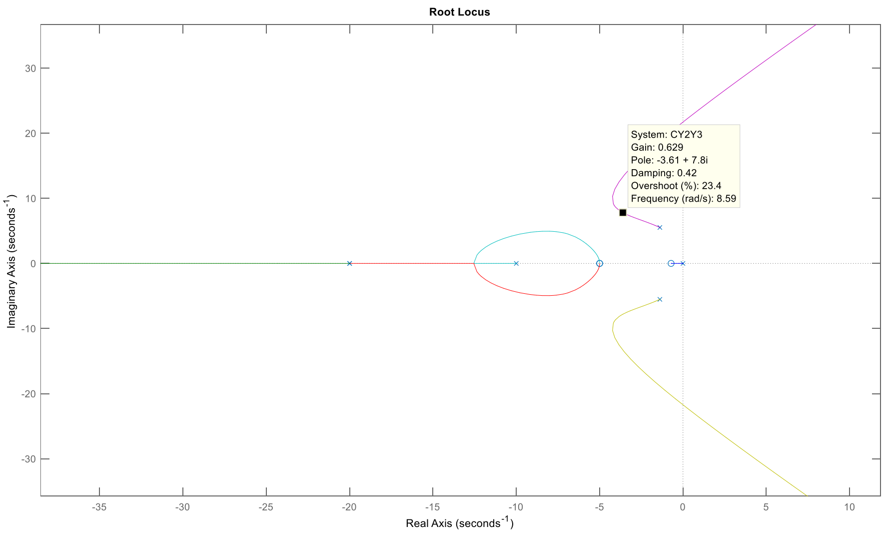

Figure 4.14 : Root-Locus diagram of inner loop controller (robust)

In above diagram, the pole and zero branches behave like the system is in stable for most conditions. The proportional gain of the controller can be chose without any doubt of unstable conditions. It is analyzed and experienced that the K gain satisfy the damping ratio with a reasonable result. In this combination of the "τ *and* C_d", K (proportional gain) can be chose as 0.629 with respect to 0.42 damping ratio, which is a good approach for a supersonic aircraft.

The difference of the first controller which is noted in Equation (4-70), and the second controller which is noted in Equation (4-71) is expressed in Figure 4.15 in terms of the time responses.

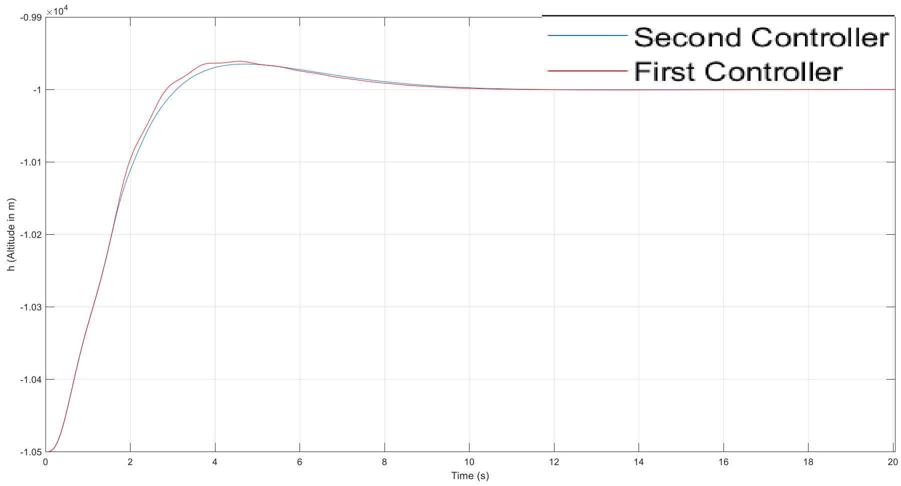

Figure 4.15 : Time response difference of first and second controller design

4.2.2.8 Outer loop controller

Since the inner loop control loop is established in a stable conditions, the outer loop of the altitude hold controller system beyond the longitudinal motion can be studied freely. For the simplicity, the closed-loop transfer function of the inner loop controller can be written as below:

$$G_{inner_{CL}}(s) = \frac{C(s)Y_2(s)Y_{\theta_{\delta e}}(s)}{1+C(s)Y_2(s)Y_{\theta_{\delta e}}(s)} = \frac{0.1813s^3+1.942s^2+5.827s+3.236}{0.0001s^6+0.0041s^5+0.0749s^4+0.786s^3+4.798s^2+15.83s+3.236} \tag{4-72}$$

The outer loop consists of the following equations:

$$\dot{h} = V_p \sin(\theta - \alpha) = V_p sin\gamma \tag{4-73}$$

Integrating the Equation (4-73) will lead to get the current altitude value of the system. When taking difference of the current and reference input of the altitude, the error is controlled with a proportional gain and feeding to the reference input of the inner control loop, which is θ_{ref}. The outer loop controller gain can be found by using the same method of the inner loop control system design. However, the inner loop is stablizing so fast. Therefore, the outer loop controller gain can be chose as the reducing the rank of the reference altitude input, since it is too big numerically with respect to the other inputs. The controller gain is chose with a constant value of 0.004 for the simplicity.

4.2.2.9 Altitude-Hold flight controller

The outer loop is designed as tracking the reference altitude input, the characteristic of the controller behaves as holding the altitude at the reference input. The total body diagram of the "Altitude-Hold Control System" is expressed in Figure 4.16:

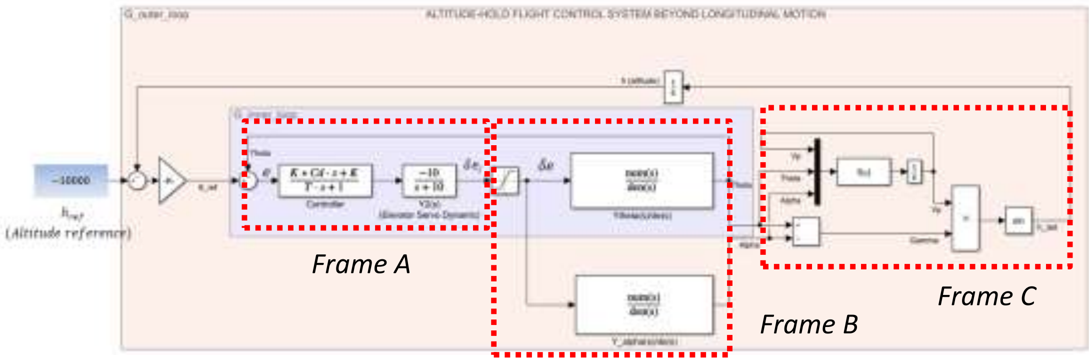

Figure 4.16 : Altitude-Hold flight control system block diagram

The Frames A,B and C, which are represented in Figure 4.17, Figure 4.18 and Figure 4.19, are shown below respectively:

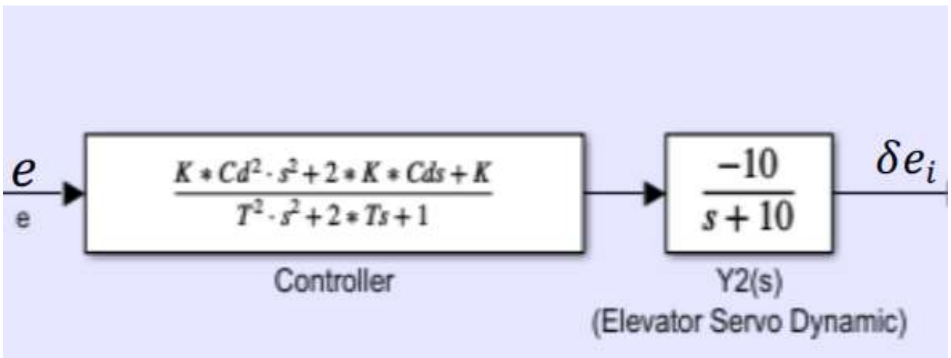

Figure 4.17 : Frame A

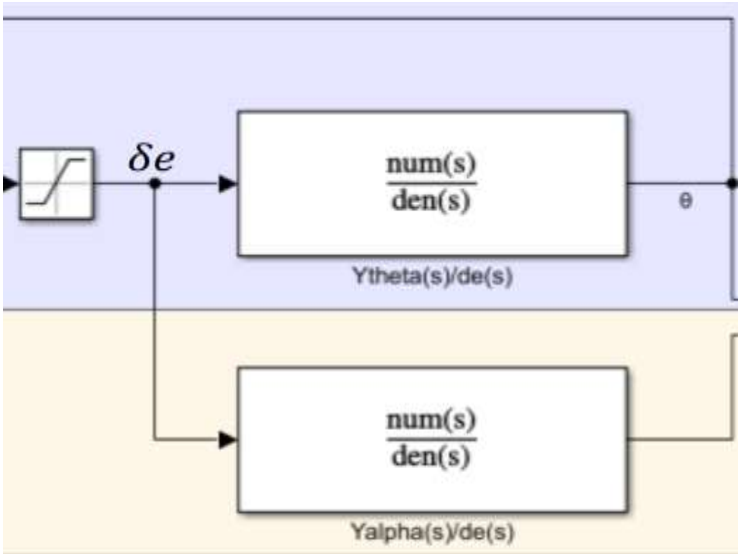

Figure 4.18 : Frame B

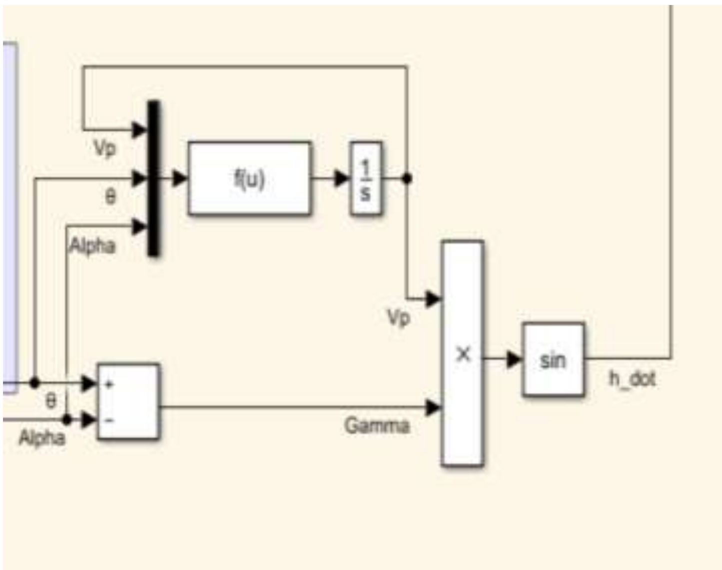

Figure 4.19 : Frame C

Following example shows that the given reference altitude is stabilized rapidly by analyzing the Figure 4.20:

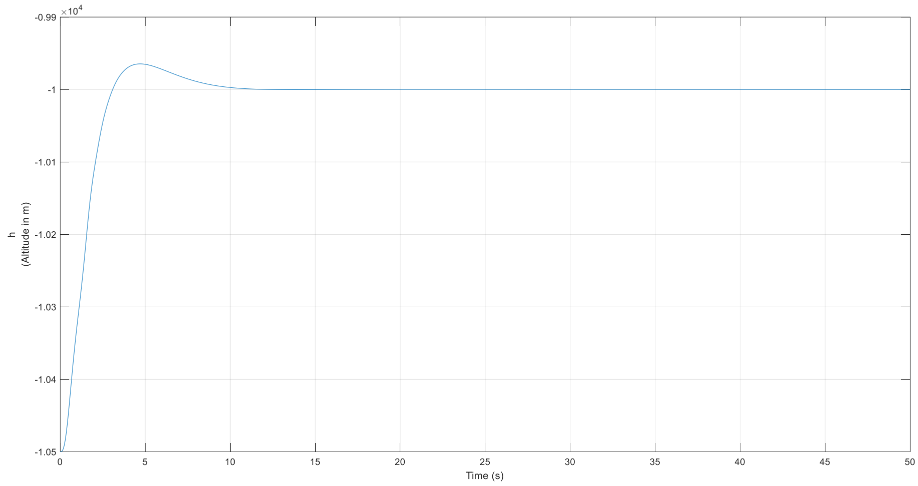

Figure 4.20 : Time response of altitude

The corresponding pitching motion angles and elevator displacement of the plant can be seen in Figure 4.21:

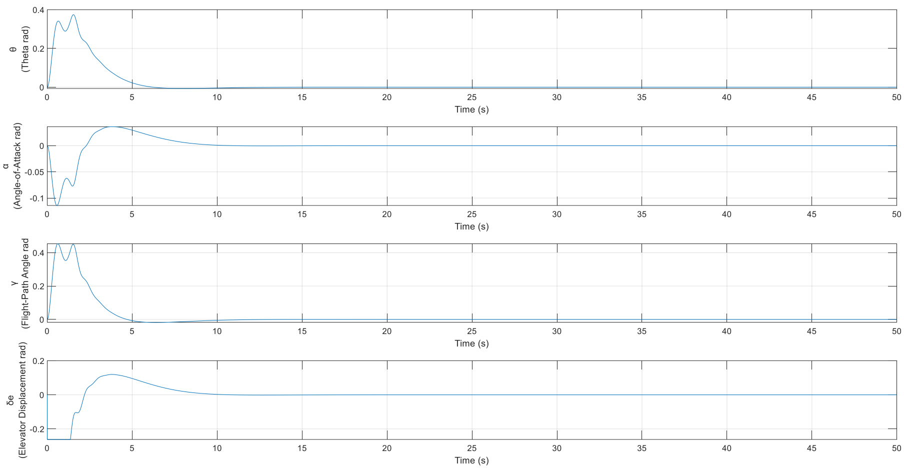

Figure 4.21 : Time response of parameters in Altitude-Hold flight control system

5. CONCLUSION

The stabilization of the short-period approximation for supersonic aircraft is completed in this study, at first. Total longitudinal airframe is linearized in order to analyze at steady, equilibrium points and to control with the conventional methods. The design of the controller is based on two stages, which are inner loop and outer loop controllers. The inner loop is dealt with making the longitudinal motion airframe steady at reference pitching motion. The controller design is completed via Root-Locus analysis. At first, a desirable controller is estimated for the current longitudinal motion airframe. Then, the proper controller gains are established by studying several controller designs according the desirable and reliable Root-Locus diagram behaviour. The suitable gains are chose to implement and complete the inner loop controller design.

The outer loop controller design is based on keeping the calculated and measured altitude of the aircraft at the reference altitude input. Therefore, the altitude motion expressions are developed and formed so that the airframe gives the calculated output for feeding back to the reference input section. The evaluating the control variable for the control method is established by choosing the proportional control gain such as the rank of the altitude is acceptable and easy to be calculated by the controller numerically.

In this study, the importance of stabilizing the short-period motion of the aircraft is experienced. The reason of using this motion of study is that it makes the aircraft moves around the critical regions. In terms of Root-Locus diagram, the steady-state response of the aircraft is close to the imaginary axis, which is critical limit of the unstable region. Therefore, the importance of stabilizing this motion leads to guaranteed stable motion of the aircraft at each longitudinal flight regimes. The other reason is that the velocity component of the airframe does not affect to the angle of attack. Hence, the derivation of the velocity does not affect to the longitudinal motion, which means that the analyzing of this motion can be easy to study. It can be worked at every flight velocity regimes.

6. FUTURE WORKS

Nonlinear Dynamic Inversion method is designed in this study. However, the model is not simulated. The future works are corresponding to the simulation of Nonlinear Dynamic Inversion method application. The results of the NDI simulation will be compared with the Altitude-Hold Flight Controller, which is built and simulated in this study.

REFERENCES

Albostan, O., 2017. High Angle of Attack Manoeuvring Control of F-16 Aircraft Based on Nonlinear Dynamic Inversion and Eigenstructure Assignment, 7th European Conference for Aeronautics and Space Sciences (EUCASS)

Blakelock, J.H., 1991. Automatic Control of Aircraft and Missiles, Wiley, 672p, New Jersey.

Gleen, B., 1978. Flight Experience with Altitude Hold and Mach Hold Autopilots on the YF-12 Aircraft at Mach 3, NASA Flight Research Center Edwards, CA, United States

Harris, J.A., 2017. Nonlinear Adaptive Dynamic Inversion Control for Variable Stability Small Unmanned Aircraft Systems, Master Thesis, Texas A&M University

Lee, D., 2020. Angle-of-Attack Command Longitudinal Control for Supersonic Advanced Trainer Aircraft, International Journal of Aeronautical and Space Sciences; https://doi.org/10.1007/s42405-020-00279-2

McLean, D., 1990. Automatic Flight Control Systems, Prentice Hall International, 610p, UK.

Miller, C.J., 2013. Nonlinear Dynamic Inversion Baseline Control Law: Architecture and Performance Predictions, NASA Dryden Flight Research Center Edwards, United States

Steer, A. J., 2004. Supersonic Transport Aircraft Longitudinal Flight Control Law Design, The Aeronautical Journal, 319p, UK

Steer, A. J., 2001. Flight Control For Advanced Supersonic Transport Aircraft Handling Quality Design, PhD Thesis, Cranfield University

Veld, R.C., 2016. Incremental Nonlinear Dynamic Inversion Flight Control, Master Thesis, Delft University of Technology

BIBLIOGRAPHY

Name-Surname : Ahmet Hulusi ÖZ

Education

High School : Oğuz Can Polat High School, 2010

Bachelor Science : Istanbul Commerce University, Faculty of Engineering, Mechatronics Engineering Department, 2012-2017

Master Science : Istanbul Commerce University, Graduate School of Natural and Applied Science, Mechatronics Engineering (English) with Thesis, 2017-2021

Publications

Öz, A. H., Kalyon, M., (2021). Altıtude-Hold Flıght Control System Design For Longitudinal Motion. İstanbul Commerce University Journal of Science, 20 (39), 19-34